Entrance channel dependence of quasifission in reactions forming ^{220}Th

R. G. Thomas,[*] D. J. Hinde, D. Duniec,[†] F. Zenke,[‡] M. Dasgupta, M. L. Brown, M. Evers,
L. R. Gasques, M. D. Rodriguez, and A. Diaz-Torres

Department of Nuclear Physics, Research School of Physical Science and Engineering,

Australian National University, Canberra, ACT 0200, Australia

Mass-angle correlations of binary fragments produced in ^{16}O + ^{204}Pb, ^{34}S + ^{186}W, and ^{48,50}Ti + ^{166,170}Er reactions have been measured for a range of bombarding energies around their Coulomb barriers. At above-barrier energies, the width of the mass distributions for the fission-like fragments in the ^{50}Ti + ^{170}Er reaction are found to be higher than those from the same compound system at similar excitation energies populated via the more mass asymmetric entrance channel reaction ^{34}S + ^{186}W, which in turn is higher than those for the ^{16}O + ^{204}Pb system. The width of the mass distributions of the Ti + Er systems is found to increase with decreasing bombarding energies, in contrast with those of the ^{16}O + ^{204}Pb and ^{34}S + ^{186}W systems, which show a monotonic reduction in mass widths. This may be associated with the elongated contact configuration at sub-barrier energies.

PACS number(s): 25.85.Ge

I. INTRODUCTION

The quasifission process [1–3], in which the system reseparates before reaching a compact compound nucleus, is a major hurdle in forming heavy and superheavy evaporation residues (ER) in heavy-ion reactions [4,5]. According to earlier dynamical models [1–3], quasifission is predicted to occur in reactions where the product of the charges $Z_1 Z_2 \geqslant 1600$. In terms of reaction time scales the quasifission process lies intermediate between the rapid deep-inelastic collisions (DIC) and the slow compound nucleus reactions. Whereas DIC are characterized by large energy dissipation with the preservation of the entrance channel mass asymmetry, quasifission involves full energy dissipation and substantial mass diffusion toward the most favorable symmetric mass split. The compound nucleus reaction, in contrast, is associated with full equilibration of all degrees of freedom. Since quasifission occurs prior to reaching a compact shape, the angular anisotropy of fission-like fragments is larger than the expectations of the transition state model (TSM) of compound nucleus fission [6–9]. Furthermore, owing to the nonequilibrium nature of the process, the mass distribution of fragments produced in quasifission can exhibit large widths and a significant correlation of fragment mass with emission angle [10–13]. These characteristics are known to depend strongly on the entrance channel [10–13]. It is expected that quasifission inhibits the formation of ER since the composite system during its dynamical evolution decays into binary fragments prior to reaching the compact compound nucleus.

The experimental evidence of quasifission in heavy-ion reactions (for projectiles with $A \geqslant 24$ on heavy targets such as ^{208}Pb) has been established from the observation of large anisotropies for fission-like fragments [6–9] and from the strong correlation between fragment mass and emission angle observed in reactions of ^{208}Pb and ^{238}U with nuclei heavier than ^{48}Ca and ^{27}Al, respectively [10–13]. The role of deformation and alignment of the heavy reaction partner in the quasifission process, particularly at sub-barrier energies, was first demonstrated experimentally in Ref. [14]. There the measured anisotropies of fission fragments in the ^{16}O + ^{238}U reaction were found to be anomalously large compared to the predictions of the TSM. This demonstrates that quasifission can be present even when the charge product is much lower than 1600 (with $Z_1 Z_2$ being a modest 736 in this case). A series of experiments by other groups followed for a range of actinide targets involving relatively lighter projectiles, all showing anomalously large fragment angular anisotropies irrespective of the entrance channel [15–17]. These results suggest that for highly fissile systems, if the heavy partner is deformed, there is an increased probability for quasifission at energies below the Coulomb barrier.

Measurements of *xn* ER cross sections have shown suppression of fusion even for less fissile compound systems, such as ^{216}Ra [18] and ^{220}Th [19], when populated by reactions involving projectiles heavier than ^{12}C and ^{16}O, respectively. For ^{220}Th, the *xn* yields imply a fusion probability of only $\sim$10% for projectiles of $A \geqslant 40$. Complete suppression of ER cross sections at sub-barrier energies was also reported for the ^{60}Ni + ^{154}Sm reaction, forming ^{214}Th [20]. The observed suppression of ER has been attributed to the presence of quasifission. If quasifission is responsible for the observed ER suppression in these reactions, evidence should be seen in the fission properties as well. In this work fission mass and angular distributions have been measured for the reactions ^{16}O + ^{204}Pb, ^{34}S + ^{186}W, and ^{50}Ti + ^{170}Er, forming ^{220}Th at the same excitation energies. Measurements for ^{50}Ti + ^{166}Er and ^{48}Ti + ^{166,170}Er were also made to confirm the very different results found for ^{50}Ti + ^{170}Er compared with the more mass-asymmetric reactions.

---

[*]Permanent address: Bhabha Atomic Research Centre, Mumbai, India.

[†]Present address: Uppsala University, P. O. Box 256, Uppsala, Sweden.

[‡]Present address: Helmholtz-Institut für Strahlen-und Kernphysik, R006, Nussallee 14–16, D-53115 Bonn, Germany.
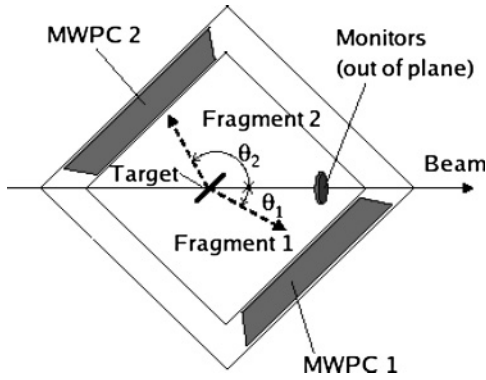
FIG. 1. Schematic of the experimental setup.

II. EXPERIMENTAL SETUP AND DATA ANALYSIS

The experiments were carried out by using beams from the 14 UD tandem accelerator of the Australian National University, operating at terminal voltages up to 15.4 MV. The detector configuration and analysis method were different for the ^{16}O, ^{34}S reactions and the ^{48,50}Ti reactions. The former are described first.

Pulsed beams of ^{16}O and ^{34}S of $\sim$1 ns width and a separation of 106 ns were used. The isotopically enriched ($> 99\%$) targets of ^{204}Pb (80 μg/cm^2 on a 20 μg/cm^2 carbon backing) and ^{186}W (50 μg/cm^2 on a 20 μg/cm^2 carbon backing) were mounted on a target ladder that was oriented at 45° to the beam direction. This eliminated shadowing of the detectors by the target frame and also minimized the energy loss of fission fragments in the target. Figure 1 shows a schematic diagram of the experimental setup. The reaction products were detected in two large-area position-sensitive multiwire proportional counters (28 cm $\times$ 36 cm), centered at polar angle $\theta = 45°$ (azimuthal angle $\phi = 90°$) (front) and $\theta = 135°$ ($\phi = 270°$) (back). The normal from the center of the detectors intersected the beam axis at a distance 18 cm from the detectors. The position of the fragment entering a detector was determined via the delay-line readout of the wire planes, giving a position resolution of better than 1 mm. The fast timing signal from the central cathode foil of each of the detectors was used to obtain the time-of-flight of the fragments with respect to the beam pulse. The target was placed 6 cm upstream along the beam direction, closer to the back detector, to increase the flight path to the front detector, which intercepts the fission fragments with the larger velocities. Two silicon monitor detectors were mounted at $\theta = \pm 22.5°$, to measure the elastic scattering flux for normalization and to obtain the absolute cross sections. The X-Y positions, the energy loss in each of the detectors, and the time of arrival of coincident fragments with respect to a given beam pulse were recorded event by event. The position calibration of the detectors was carried out using the known positions of the edges of the illuminated areas of the detectors when the events were collected in noncoincidence mode. The calibrated X and Y positions from the two detectors were then converted to θ and ϕ. By using these angles and the time-of-flight information the fragment velocities were determined. The velocity vectors $\vec{v}_1$ and $\vec{v}_2$ in the laboratory frame of reference of the masses m_1 and m_2

were reconstructed for coincident fragments after correcting for the energy loss suffered by the fragments in the target, under the assumption that the interactions take place at the midpoint of the target. It is found that, as the targets used were thin, this correction affects the derived mass ratios by less than 2%. The effect of energy loss in the detector windows (0.9 μm PET) was neglected, as the flight path from window to detector was only 10% of the total. This means that the correction to the mass ratios is typically $\ll 1\%$, which is not significant in this work.

The corrected velocities were then converted to the center-of-mass frame by applying kinematic transformations using the calculated value of the center-of-mass velocity $\vec{V}_{\text{c.m.}}$ rather than its experimentally deduced value $\vec{V}_\|$. This was done because the emission of light particles from the compound system perturbs the fission fragment velocity vectors, resulting in a significant spread in $\vec{V}_\|$ when the angles θ_1 and θ_2 are close to 0° and 180°, which in turn can affect the deduced mass ratios [21]. From the center-of-mass velocities $\vec{v}_{1\text{c.m.}}$ and $\vec{v}_{2\text{c.m.}}$ of the two fragments, using linear momentum conservation,

$$m_1 \vec{v}_{1\text{c.m.}} = m_2 \vec{v}_{2\text{c.m.}}, \qquad (1)$$

we obtain the mass ratio

$$M_R = \frac{m_2}{m_1 + m_2} = \frac{\vec{v}_{1\text{c.m.}}}{\vec{v}_{1\text{c.m.}} + \vec{v}_{2\text{c.m.}}}. \qquad (2)$$

The determination of the time zero for the time-of-flight spectrum for each energy was done by imposing two conditions: (a) Setting the average $\vec{V}_\| = \vec{V}_{\text{c.m.}}$ and (b) ensuring that the M_R distribution is reflection symmetric about 0.5 at all angles for the ^{16}O induced reaction, as this reaction is expected to be a true compound nucleus reaction. Condition (a) determines the time shift between the RF signal and the beam burst and hence varies with the beam energy, whereas condition (b) determines the constant electronic time delay between the two detectors and is independent of beam energy. The measured fission $\vec{V}_\|$ distributions were symmetric about $\vec{V}_{\text{c.m.}}$, and consistent with those for elastic scattering (where observed), showing that the fission events followed full projectile momentum transfer, with no significant contribution from fission following incomplete fusion.

Measurements for the Ti + Er reactions were carried out by using the same detectors. However, because of the increased forward-focusing of the fission fragments in these reactions, the geometry of the setup was different from that just described, with the back detector (MWPC 2) being centered at $\theta = 90°$ ($\phi = 270°$). The isotopically enriched targets ($\sim$100 μg/cm^2 on $\sim$12 μg/cm^2 carbon backings) were mounted on a target ladder, positioned at the geometrical center and oriented at 30° relative to the beam direction. Moreover, owing to the low abundance of ^{50}Ti in natural titanium (only 5%), a DC beam was used and the time difference between the detector time signals was recorded instead of the time of flight of each detector. The measurement of time difference [22] obviated the need for a pulsed beam, resulting in higher beam intensity and better statistics. A potential drawback of the time difference method (applied only for the ^{50}Ti $+^{170}$Er reaction) is the intrinsic assumption of a strictly binary reaction
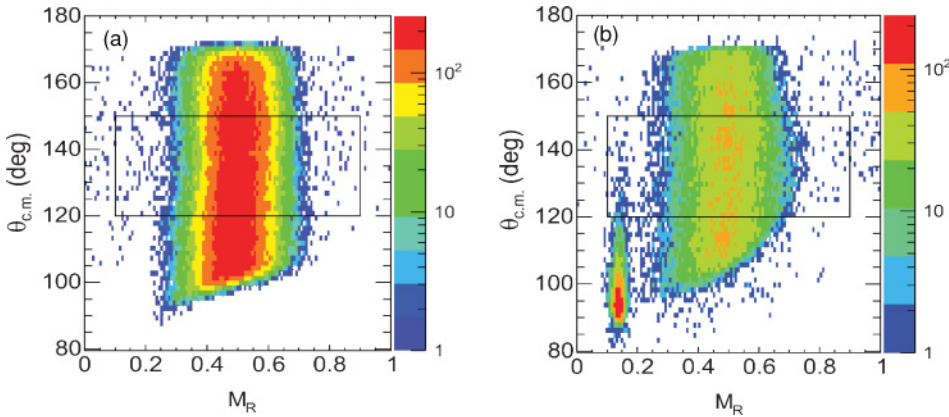
FIG. 2. (Color online) The mass ratio vs center-of-mass angle density plot for the (a) ^{16}O + ^{204}Pb and (b) ^{34}S + ^{186}W systems at $E_{lab} = 126.0$ and 188.9 MeV, respectively.

when deducing the mass ratios. Since the target used in this experiment was not fissile, the probability of nonbinary events such as transfer-induced fission is expected to be negligibly small, and the assumption is justified in this case. For one measurement, a DC beam of ^{48}Ti was used to verify that the time difference analysis gave the same result as the absolute time analysis.

The time difference calibration for the system was achieved by imposing the condition that the M_R distribution of fission-like events is reflection symmetric about 0.5 at $\theta_{c.m.} = 90°$, a condition that is true for all reactions. The solid angle calibration of the detectors was done by measuring elastic scattering in the ^{50}Ti + ^{197}Au reaction at a sub-barrier energy $E_{lab} = 160$ MeV. The velocities and the mass distributions were reconstructed from the position and time difference information as described in the Appendix.

III. RESULTS AND INTERPRETATION

A. Mass-angle correlations

Figure 2 shows M_R versus center-of-mass angle spectra for the ^{16}O + ^{204}Pb and ^{34}S + ^{186}W reactions, and Fig. 3 shows the same plot for ^{48}Ti + ^{170}Er. The fission-like fragments are centered around $M_R = 0.5$, and the geometry of the detector setup limits the most forward and backward events for a
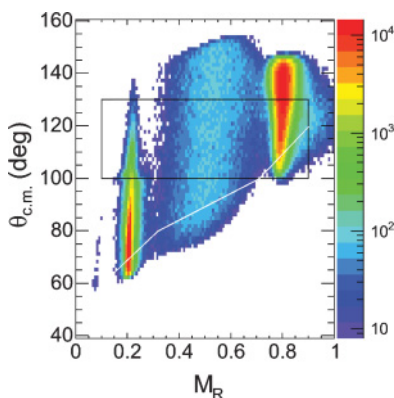

FIG. 3. (Color online) Same as Fig. 2 but for the ^{48}Ti + ^{170}Er system at $E_{lab} = 245.0$ MeV.

given mass ratio. A cut in the azimuthal angle ($\Delta\phi = 70°$) was imposed so that the counts at any given angle θ are proportional to $\frac{d\sigma}{d\theta}$. The projectile-like fragments [left-hand group in Fig. 2(b) and Fig. 3] can be seen for the ^{34}S- and ^{48}Ti-induced reactions. The target-like fragments can also be seen on the right-hand side in Fig. 3 for the case of ^{48}Ti + ^{170}Er. However, in the ^{16}O-induced reaction, neither of these groups (projectile-like and target-like) are seen because of the combined effect of the geometry of the setup, the reaction kinematics, and detector thresholds. The rectangles shown in the figures represent the gates used to obtain the mass ratio spectra shown in Sec. III B. They were chosen so as to avoid biasing of the data from the geometric limitations of the experimental setup.

Although there is little or no dependence of mass ratio on the center-of-mass angle in the case of ^{16}O + ^{204}Pb and ^{34}S + ^{186}W, the ^{48}Ti + ^{170}Er reaction shows a strong correlation of mass ratio with emission angle. Since the mass-angle correlation for the ^{48}Ti + ^{170}Er reaction extends forward of 90°, we can generate the full mass-angle correlation by transposing [i.e., $\theta_{c.m.} \rightarrow \pi - \theta_{c.m.}$ and $M_R \rightarrow (1 - M_R)$] the distribution in Fig. 3 across the white line. This is shown in Fig. 4 and is helpful in illustrating the strong forward-backward asymmetry of fission-like fragments in the Ti + Er reactions. It can also be seen that the correlation of mass with angle is present at the highest [Fig. 4(a)] as well as at the lowest [Fig. 4(b)] energies studied.

This strong correlation suggests a contribution from quasifission at all mass ratios and is in agreement with the results of Ref. [23] for ^{48}Ti + ^{166}Er, where fragment masses were measured in singles by using energy and time information. Our recent measurements [24] also show a significant mass-angle correlation for the ^{48}Ti + ^{154}Sm reaction. These results differ from the experimental measurements for the reactions ^{48}Ca + ^{168}Er [25] and ^{48}Ca + ^{154}Sm [26], measured by using a similar kinematic coincidence method as that of the current work. In the latter measurements, with a ^{48}Ca projectile, it is only the extreme mass-asymmetric components that are attributed to quasifission. The physical origin of this difference needs detailed experimental investigation, as it may be due to nuclear structure effects influencing the fusion dynamics.

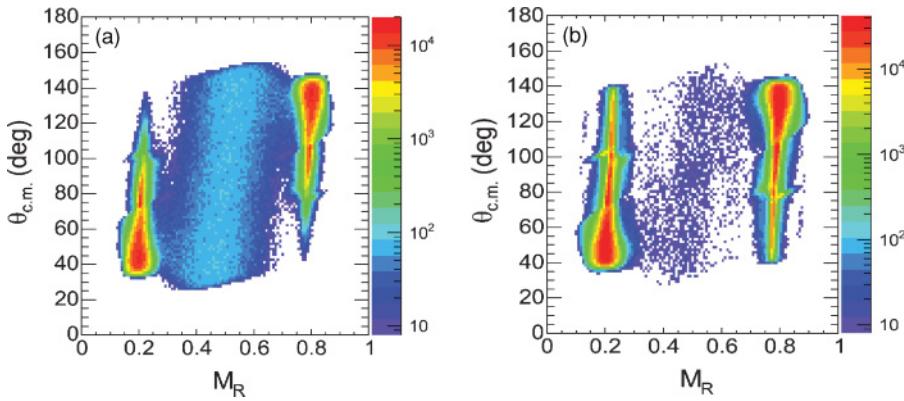It should be noted that when a mass-angle correlation is present, applying symmetrization of the distribution about

FIG. 4. (Color online) The mass ratio vs center-of-mass angle density plot for the ^{48}Ti$+^{170}$Er system at (a) $E_{\mathrm{lab}} = 245.0$ MeV and (b) $E_{\mathrm{lab}} = 208.0$ MeV.

$M_R = 0.5$ can lead to incorrect mass distributions. This is illustrated in Fig. 5, where the mass distribution ($M_R < 0.5$) in Fig. 4(a) is reflected across $M_R = 0.5$. Comparison with Fig. 4(a) illustrates that the mass ratio distribution in Fig. 5 shows a fictitious increase in width with decreasing $\theta_{\mathrm{c.m.}}$. However, in cases where there is no mass-angle correlation (Fig. 2) or if the measurement is done at $\theta_{\mathrm{c.m.}} = 90°$, symmetrization about $M_R = 0.5$ should not yield incorrect distributions.

B. Mass ratio distributions in reactions forming ^{220}Th

To eliminate the distortion of mass ratio spectra by the geometrical acceptance of the detectors, a window in $\theta_{\mathrm{c.m.}}$ ($120°–150°$) was chosen for the ^{16}O$+^{204}$Pb and ^{34}S$+^{186}$W reactions as shown in Fig. 2. For the Ti + Er reactions, the detector acceptance did not extend beyond $140°–145°$; thus a window of $100°–130°$ was used (see Fig. 3). Figure 6 shows the mass ratio distributions of fission-like fragments of the three reactions leading to the same compound nucleus ^{220}Th. As can be seen the mass ratio distributions for the ^{16}O$+^{204}$Pb and ^{34}S$+^{186}$W reactions can be well described by Gaussians centered at $M_R = 0.5$ at all the energies, whereas the distributions in the ^{50}Ti$+^{170}$Er reaction tend to increasingly deviate from a symmetric Gaussian with decreasing bombarding energy. Though fitting a Gaussian function to a mass distribution that is not angle integrated is not well justified in cases where
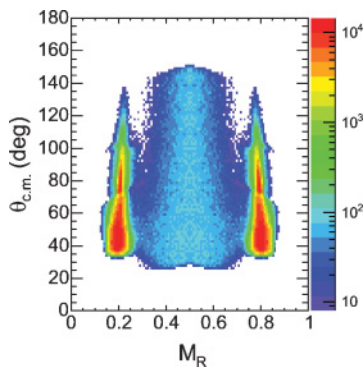

FIG. 5. (Color online) Mass ratio vs center-of-mass angle density plot for the ^{48}Ti$+^{170}$Er system at $E_{\mathrm{lab}} = 245.0$ MeV when reflected about $M_R = 0.5$.

there is significant correlation of mass with emission angle, the Gaussian fit parameters allow a simple characterization of the M_R distributions as a function of bombarding energy and the compound nucleus excitation energy.

The standard deviations (σ_M) of the Gaussian fits to the mass ratio distributions are plotted as a function of the compound nucleus excitation energy in Fig. 7. The ^{16}O$+^{204}$Pb reaction shows the expected increase in σ_M as a function of increasing compound nucleus excitation energy, E^*. The more symmetric reaction, ^{34}S$+^{186}$W, also shows similar behavior, but the magnitude of σ_M is higher than in the ^{16}O$+^{204}$Pb case over the entire range of excitation energies. It is known that σ_M^2 depends weakly on $\langle l^2 \rangle$, where l is the angular momentum brought in by the projectile [26–28]. To show that this weak dependence is not responsible for the observed difference in σ_M for the three cases, we plot in Fig. 8 the variation of $\langle l^2 \rangle$ of the compound system as a function of E^* for the three systems, as predicted by the coupled channel code CCFULL [29]. The parameters for the coupled channel calculations were chosen so as to match the average experimentally determined fusion barrier of the respective systems. The thin dotted line represents the corresponding l at which the macroscopic liquid-drop fission barrier [30] becomes equal to 1 MeV: At angular momenta higher than this value, fast fission, a process in which the system reseparates owing to the negligible fission barrier height at high angular momentum, can occur. The l values for all three reactions in the energy range studied are less than this limiting l, which rules out the possibility of fast fission. It can be seen from Fig. 8 that at E^* close to 47.5 MeV the ^{16}O$+^{204}$Pb and ^{34}S$+^{186}$W reactions have the same $\langle l^2 \rangle$ but the difference in σ_M still persists, pointing to the presence of quasifission in the latter system. This fact is also consistent with the observation of increased contribution of quasifission with decreasing mass asymmetry, as concluded by Berriman *et al.* [18], even for relatively light projectile-target systems. For the ^{50}Ti$+^{170}$Er reaction, the behavior of σ_M is qualitatively different. It is larger than the σ_M for the ^{34}S$+^{186}$W reaction, indicating a continuing evolution toward quasifission for the ^{50}Ti projectile, but in contrast with the other reactions σ_M increases as E^* decreases. This feature observed in the ^{50}Ti$+^{170}$Er reaction is also found for the reactions ^{48}Ti$+^{166,170}$Er and ^{50}Ti$+^{166}$Er, as shown in Sec. III C. Mass widths for the reactions ^{32}S$+^{182}$W and ^{48}Ti$+^{166}$Er were reported in Ref. [23]. Although not highlighted in that work,
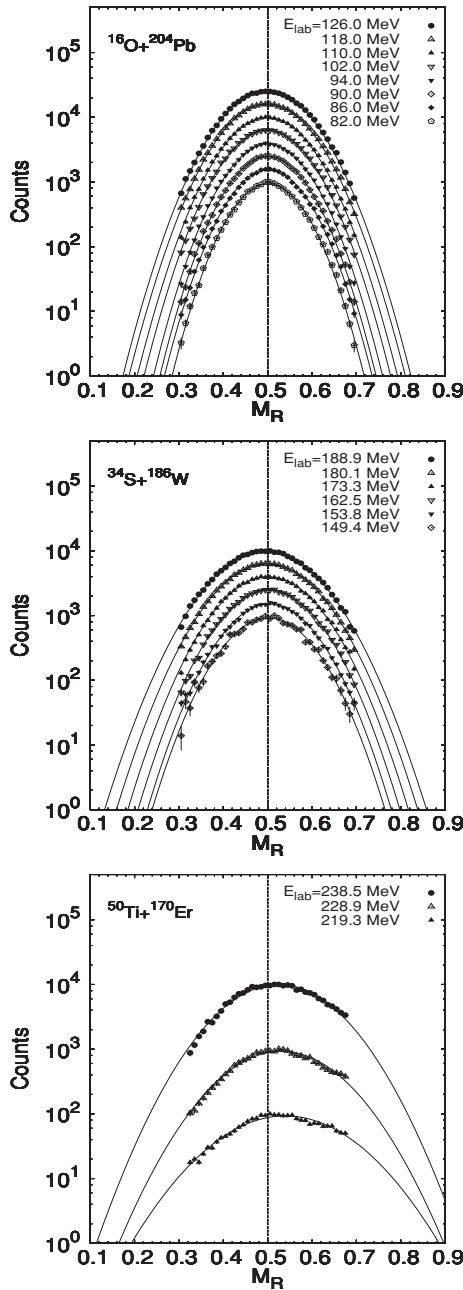
FIG. 6. The mass ratio distributions for the three systems leading to ^{220}Th. Note that the distribution tends to deviate from a symmetric Gaussian distribution for the ^{50}Ti $+^{170}$Er reaction particularly at the lowest energy.

in the same energy range as the current measurements they show the same detailed features, namely a larger mass width for Ti than for S and an increase in mass width for Ti at the lowest (near-barrier) energy. The latter feature, observed more clearly in the current work, may well be associated with the static deformation of ^{170}Er and its alignment at sub-barrier energies, as discussed in detail in the next section.

C. Mass ratio distributions in ^{48,50}Ti $+ ^{166,170}$Er reactions

Figure 9 shows the mass ratio distributions for the ^{48}Ti $+^{170}$Er and ^{50}Ti $+^{170}$Er reactions at similar compound
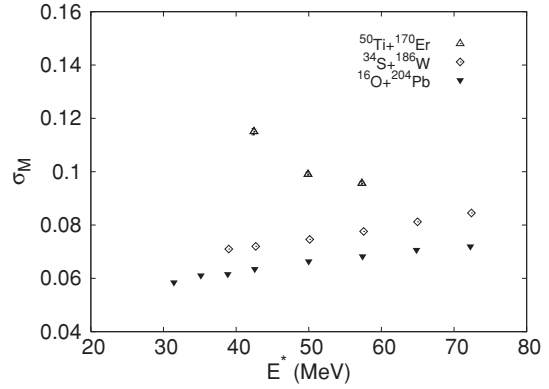

FIG. 7. The standard deviation of the Gaussian fit to the mass distribution of the fission-like fragments as a function of the compound nucleus excitation energy for the ^{220}Th system populated by three different entrance channels.

nucleus excitation energies of 40.4 and 42.5 MeV, respectively. The elastic/deep-inelastic peaks are shown to illustrate the experimental mass resolution. From their widths, taking into account the lower fission fragment velocities, the FWHM of the instrumental mass ratio resolution for the fission events is expected to be <0.02. The shoulders seen in the mass ratio distribution (at $M_R = 0.35$ and 0.65) of the ^{48}Ti $+^{170}$Er reaction seem to be associated with the presence of a quasifission component that has a large forward-backward asymmetry [see Fig. 4(b)]. This feature in quasifission has been observed in ^{238}U-induced reactions on ^{32}S and heavier targets [13]. One may argue that the effect of shell structure on the potential energy surface must cause these structures in the mass distributions. However, in the ^{50}Ti $+^{170}$Er reaction, which differs only by two neutrons and has similar excitation energy, only weak evidence of structures is observed in the mass distribution. Thus the origin of the observed structures for the ^{48}Ti $+^{170}$Er system is not yet clear, and more evidence needs to be obtained.

The systematic variation of the experimental quantities may give significant information on the reaction dynamics. The
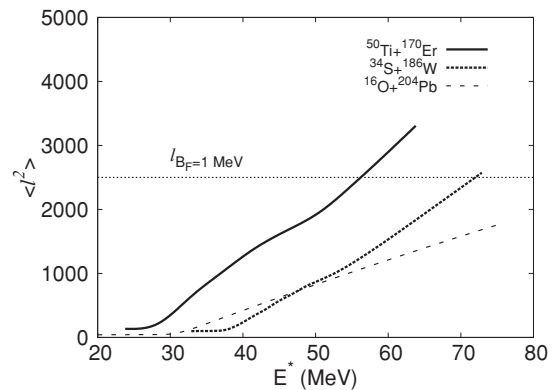

FIG. 8. Variation of $\langle l^2 \rangle$ as a function of the compound nucleus excitation energy, as predicted by the coupled channel code CCFULL [29], for the ^{220}Th system populated by three different entrance channels. The thin dotted line shows the critical angular momentum value at which the liquid drop barrier becomes equal to 1 MeV.
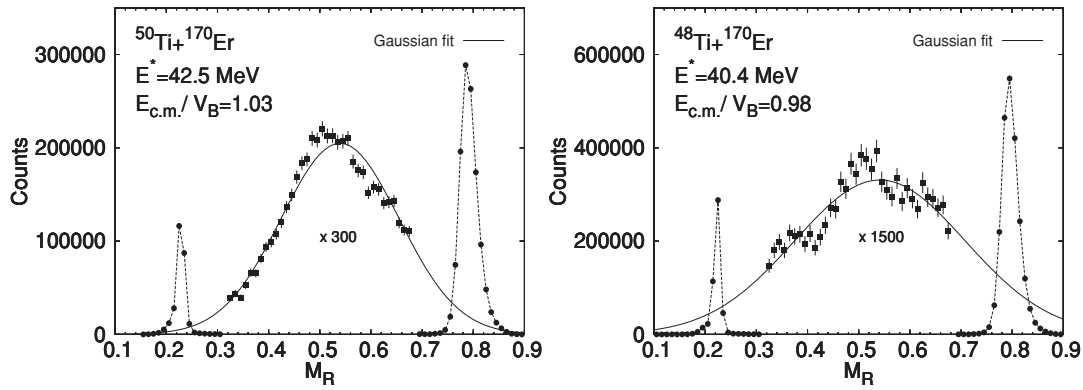
FIG. 9. The mass ratio distributions for ^{50}Ti$+^{170}$Er and ^{48}Ti$+^{170}$Er systems at similar compound nucleus excitation energies. The elastic/deep-inelastic peaks show the experimental mass resolution.

σ_M values deduced from the Gaussian fits to the mass distributions are plotted as a function of the compound nucleus excitation energy in Fig. 10(a) for all the Ti + Er reactions in the present study. Figure 10(b) illustrates the dependence of σ_M on the ratio of bombarding energy to the fusion barrier for all the Ti + Er systems as well as those of ^{16}O + ^{204}Pb
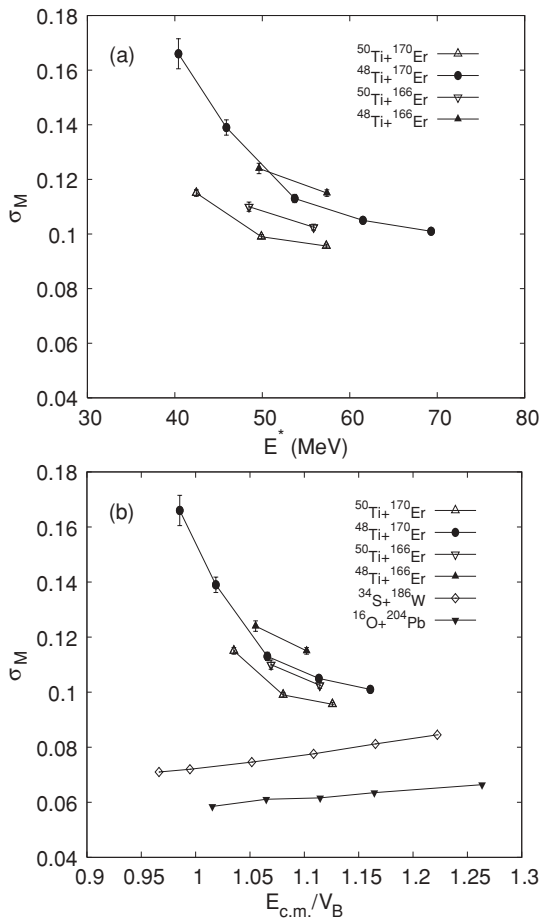

FIG. 10. (a) The standard deviation σ_M of the fission-like fragments ($M_R = 0.3$–0.7) as a function of the compound nucleus excitation energy and (b) as a function of center-of-mass energy with respect to the Coulomb barrier.

and ^{34}S $+^{186}$W systems. The σ_M values for all the Ti + Er reactions show a closely correlated rise with decreasing E^* as well as $E_{c.m.}/V_B$, but in neither case do the data for the different Ti + Er reactions collapse onto a single curve. This observation for these reactions suggests that the rise in width with decreasing beam energy should not immediately be associated either with E^* or with $E_{c.m.}/V_B$ without a more detailed analysis, which is given below.

The difference in σ_M values for the different Ti + Er reactions may be related to the difference in fissility resulting from the difference in the number of neutrons. To check this, we plot σ_M against the mean fissility χ_m of the composite system for each of the Ti + Er reactions, where $\chi_m = \frac{2}{3}\chi + \frac{1}{3}\chi_e$ [2,3]. The mean fissility represents the degree of re-separability of the dinuclear system, which is macroscopically determined by the Coulomb repulsion in the initial stage of the reaction (χ_e) and the balance between the Coulomb and the surface energies (χ) of the compound nucleus in the later stage of the reaction. It is known that the onset of quasifission is strongly dependent on the mean fissility [3]. The calculated extra-extra-push energy (the excess energy over the interaction barrier to achieve fusion in heavy systems) shows a dramatic rise [3] at χ_m around 0.73, indicating a rapid onset of quasifission or increase in the probability of quasifission as a function of χ_m. Figure 11(a) shows the interpolated values of σ_M, taken from Fig. 10(a), as a function of χ_m at two different compound nucleus excitation energies for the Ti + Er systems. There is a discontinuous dependence for a fixed E^*, which would not be expected, as possible shell effects should be insignificant by $E^* = 50$ MeV. Figure 11(b) shows the interpolated values of σ_M, taken from Fig. 10(b), as a function of χ_m for $E_{c.m.}/V_B = 1.1$ and 1.065. Here, in contrast, a smooth increase of σ_M with χ_m is found for a fixed $E_{c.m.}/V_B$. This correlation between σ_M and χ_m is likely to correspond to an increasing contribution of quasifission with χ_m, which is what would qualitatively be expected. The smooth trend of σ_M with χ_m, found only when the data are selected on the basis of $E_{c.m.}/V_B$, strongly indicates that it is the beam energy with respect to the barrier that is the key variable determining the characteristics of the observed mass distributions, as previously suggested for the ^{32}S $+^{232}$Th reaction [31]. It would be interesting to see whether such a
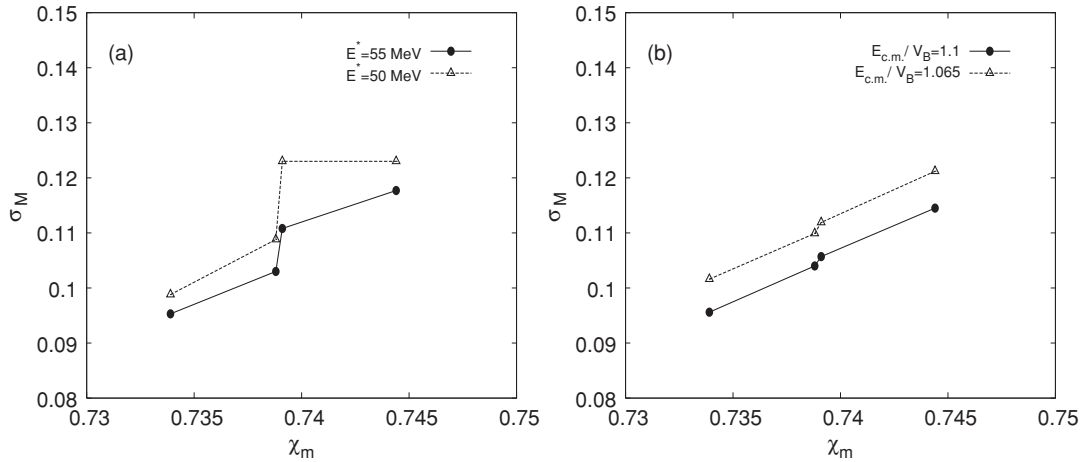
FIG. 11. The dependence of σ_M on the mean fissility (χ_m) of the composite system (a) at a given excitation energy of the compound nucleus and (b) at a given excess energy over the barrier for the Ti + Er reactions.

correlation exists at bombarding energies below the barrier, since nuclear structure effects that may strongly influence the onset of quasifission [21,31] are not taken into account in the parameter χ_m. More extensive sub-barrier measurements would be needed for such a study.

D. Reaction time and mass widths

Although both the target nuclei ^{186}W and ^{170}Er are statically deformed, the dramatically different behavior of their mass ratio distributions clearly shows differences in the complex evolution of the trajectories of the composite system over the multidimensional potential energy surface, implying a strong dependence on the entrance channel conditions. It is well known that the dynamical evolution of trajectories is strongly dependent on the charge product $Z_1 Z_2$ (or more specifically on χ_e) of the dinuclear system [1–3]. Though the unconditional saddle point elongation of the three systems forming the ^{220}Th nucleus is the same, from the experimental observations, one may postulate that only in the case of the lightest system, ^{16}O + ^{204}Pb where the product $Z_1 Z_2$ is 656, are the trajectories reaching a fully equilibrated compound nucleus. This is supported by the analysis of angular distribution measurements done earlier for a similar system, ^{16}O + ^{208}Pb [32], which were quite consistent with a fusion-fission process. However, the ^{34}S + ^{186}W system, which has a moderate $Z_1 Z_2$ value of 1184, shows signs of reseparation (quasifission) before reaching full mass equilibration, as is evident from the larger σ_M value. Nonetheless, the system must remain together longer than the empirically determined time constant τ_M ($\sim 5 \times 10^{-21}$ s) for mass equilibration [13] and complete several rotations before reseparation, as there is no experimental evidence of any significant correlation of M_R with emission angle (Fig. 2). However, the large anisotropies observed for a very similar system, ^{32}S + ^{182}W [23,33], points to the fact that the system reseparates before full relaxation of the K degree of freedom (the tilting mode), which has a longer empirical equilibration time ($\tau_K \sim 10^{-20}$ s) [17,34–36]. For the ^{50}Ti + ^{170}Er system, with a high $Z_1 Z_2$ value of 1496, the trajectories over the potential energy surface are evidently

more likely to be deflected away from compact configurations owing to the larger Coulomb repulsion, with a substantial portion escaping before reaching the bottom of the mass-symmetric fission valley. The strong correlation of M_R with angle indicates that the system reseparates even before a full rotation, with reaction times shorter than τ_M.

It is quite apparent that the experimental observables in quasifission reactions are found to crucially depend on the interaction time (sticking time [3]) of the dinuclear complex with respect to the characteristic relaxation time of various degrees of freedom, before it decays into binary fission-like fragments. This interaction time in turn depends on the entrance channel parameters of the colliding nuclei. Thus a system that remains together for a time comparable or shorter than τ_M exhibits strong mass-angle correlations, large mass widths, and large anisotropies. Systems whose sticking time is between τ_M and τ_K may not show any significant correlation of mass with angle but can show broadened mass distributions and large angular anisotropies. However, systems that stick together for time scales comparable to τ_K but reseparate before reaching a compound nucleus may not exhibit any signs of incomplete relaxation of mass but can still exhibit angular anisotropies larger than predicted by the TSM for compound nucleus fission.

IV. SUMMARY AND CONCLUSIONS

Mass-angle correlations have been measured at energies around the Coulomb barrier for three reactions, ^{16}O + ^{204}Pb, ^{34}S + ^{186}W, and ^{50}Ti + ^{170}Er, which form the ^{220}Th nucleus at similar excitation energies. Measurements were also carried out for the ^{50}Ti + ^{166}Er and ^{48}Ti + ^{166,170}Er reactions. At above-barrier energies, the widths of the mass distributions for the fission-like fragments in the ^{50}Ti + ^{170}Er reaction are found to be higher than those for the more mass-asymmetric entrance channel reaction ^{34}S + ^{186}W, which in turn are higher than those in the ^{16}O + ^{204}Pb system. This suggests that the more symmetric entrance channel combinations, ^{34}S + ^{186}W and ^{50}Ti + ^{170}Er, show evidence of quasifission compared to the asymmetric ^{16}O + ^{204}Pb reaction.

It is found that the width of the mass distributions in the Ti + Er reactions increases as a function of decreasing bombarding energy, in contrast with those of the ^{16}O + ^{204}Pb and ^{34}S + ^{186}W systems, which show a monotonic reduction in mass widths with decrease in energy. This is interpreted as a strong dependence of the reaction dynamics on the orientation of the deformed ^{170}Er nucleus [14,21].

The mass ratio distributions of the Ti + Er reactions show incomplete mass equilibration, clearly evident from the large mass widths. They also show a dependence on the center-of-mass angle, indicating the presence of fission-like events occurring on a time scale comparable to that of the rotation time of the dinuclear complex. The ^{34}S + ^{186}W system, in contrast, shows signs of fission before full mass equilibration through the larger value of σ_M as compared to the ^{16}O + ^{204}Pb system. However, the negligible dependence of M_R on the emission angle indicates that the system typically reseparates after a time sufficient to complete one or more rotations. A significant dependence of σ_M on the mean fissility, χ_m, is also noticed among the Ti + Er reactions, suggesting that the quasifission probability increases as a function of χ_m at a given ratio of bombarding energy to fusion barrier energy. The dependence of the quasifission probability on the entrance channel parameters such as mass asymmetry, $Z_1 Z_2$, static deformation, and orientation of the colliding nuclei needs to be incorporated in any dynamical model that aims to quantitatively predict the production probability of heavy and superheavy elements. More systematic studies of the dependence of quasifission as a function of these entrance channel variables in different regions of fissility may be helpful in determining which are the key variables to incorporate in such a model. The model should be tested not only by reproducing the production probability of heavy evaporation residues in heavy-ion reactions but also by describing the properties of binary fragmentation as well.

APPENDIX

For completeness we describe our determination of the mass ratio from the time difference between the members of the fragment pair entering the detectors. If θ_1 and θ_2 are the polar angles with respect to the beam direction of the fragments m_1 and m_2, respectively, with the assumption of full momentum transfer, we have [22]

$$p_1 \cos(\theta_1) + p_2 \cos(\theta_2) = m_{CN} V_{CN} \qquad (A1)$$

and

$$p_1 \sin(\theta_1) = p_2 \sin(\theta_2), \qquad (A2)$$

from which it follows that

$$p_1 = \frac{m_{CN} V_{CN}}{\cos(\theta_1) + \sin(\theta_1)\cot(\theta_2)} \qquad (A3)$$

and

$$p_2 = \frac{p_1 \sin(\theta_1)}{\sin(\theta_2)}, \qquad (A4)$$

where p_1 and p_2 are the momenta of the two fragments and V_{CN} is the velocity of the compound system.

The time-of-flight difference between the fragments entering the two detectors can be written as

$$t_1 - t_2 = \frac{d_1}{v_1} - \frac{d_2}{v_2} = \frac{d_1 m_1}{p_1} - \frac{d_2}{p_2}(m_{CN} - m_1), \qquad (A5)$$

where $m_1 + m_2 = m_{CN}$.

Equation (A5) can be simplified to yield

$$m_1 = \frac{(t_1 - t_2) + \delta t_0 + m_{CN}\frac{d_2}{p_2}}{\frac{d_1}{p_1} + \frac{d_2}{p_2}}, \qquad (A6)$$

where d_1 and d_2 are the flight paths of the masses m_1 and m_2, respectively, and the additional factor δt_0 is the electronic delay between the timing signals of the two detectors. The constant factor δt_0 for a given experimental setup is obtained by the calibration procedure described in the text. It is worth mentioning that this method does not allow good discrimination between fission resulting from full momentum transfer and fission following transfer reactions, owing to the assumption of full momentum transfer.

[1] W. J. Swiatecki, Phys. Scr. **24**, 113 (1981).
[2] S. Bjornholm and W. J. Swiatecki, Nucl. Phys. **A391**, 471 (1982).
[3] J. P. Blocki *et al.*, Nucl. Phys. **A459**, 145 (1986).
[4] Yu. Ts. Oganessian and Yu. A. Lazarev, in *Treatise on Heavy-Ion Science*, Vol. 4, edited by D. A. Bromley (Plenum Press, New York, 1985), p. 3.
[5] P. Armbruster, C. R. Phys. **4**, 571 (2003).
[6] B. B. Back *et al.*, Phys. Rev. Lett. **50**, 818 (1983).
[7] M. B. Tsang *et al.*, Phys. Lett. **B129**, 18 (1983).
[8] K. T. Lesko, S. Gil, A Lazzarini, V. Metag, A. G. Seamster, and R. Vandenbosch, Phys. Rev. C **27**, 2999 (1983).
[9] B. B. Back *et al.*, Phys. Rev. C **32**, 195 (1985).
[10] R. Bock *et al.*, Nucl. Phys. **A388**, 334 (1982).
[11] J. Toke *et al.*, Phys. Lett. **B142**, 258 (1984).
[12] J. Toke *et al.*, Nucl. Phys. **A440**, 327 (1985).
[13] W. Q. Shen *et al.*, Phys. Rev. C **36**, 115 (1987).
[14] D. J. Hinde *et al.*, Phys. Rev. Lett. **74**, 1295 (1995).
[15] Z. Liu *et al.*, Phys. Lett. **B353**, 173 (1995).
[16] J. C. Mein, D. J. Hinde, M. Dasgupta, J. R. Leigh, J. O. Newton, and H. Timmers, Phys. Rev. C **55**, R995 (1997).
[17] J. P. Lestone, A. A. Sonzogni, M. P. Kelly, and R. Vandenbosch, Phys. Rev. C **56**, R2907 (1997).
[18] A. C. Berriman *et al.*, Nature (London) **413**, 144 (2001).
[19] D. J. Hinde, M. Dasgupta, and A. Mukherjee, Phys. Rev. Lett. **89**, 282701 (2002).
[20] S. Mitsuoka, H. Ikezoe, K. Nishio, and L. Lu, Phys. Rev. C **62**, 54603 (2000).
[21] D. J. Hinde, M. Dasgupta, J. R. Leigh, J. C. Mein, C. R. Morton, J. O. Newton, and H. Timmers, Phys. Rev. C **53**, 1290 (1996).
[22] R. K. Choudhury *et al.*, Phys. Rev. C **60**, 054609 (1999).

[23] B. B. Back *et al.*, Phys. Rev. C **53**, 1734 (1996).

[24] R. Rafiei *et al.*, Phys. Rev. C **77**, 024606 (2008).

[25] A. Yu. Chizhov *et al.*, Phys. Rev. C **67**, 011603(R) (2003).

[26] G. N. Knyazheva *et al.*, Phys. Rev. C **75**, 064602 (2007).

[27] M. G. Itkis and A. Ya. Rusanov, Phys. Part. Nuclei **29**, 160 (1998).

[28] E. G. Ryabov *et al.*, Nucl. Phys. **A765**, 39 (2006).

[29] K. Hagino *et al.*, Comput. Phys. Commun. **123**, 143 (1999).

[30] A. J. Sierk, Phys. Rev. C **33**, 2039 (1986).

[31] D. J. Hinde *et al.*, Nucl. Phys. **A685**, 72c (2001).

[32] C. R. Morton *et al.*, Phys. Rev. C **52**, 243 (1995).

[33] J. G. Keller *et al.*, Phys. Rev. C **36**, 1364 (1987).

[34] K. Lutzenkirchen *et al.*, Z. Phys. A **320**, 529 (1985).

[35] V. S. Ramamurthy and S. S. Kapoor, Phys. Rev. Lett. **54**, 178 (1985).

[36] R. G. Thomas, R. K. Choudhury, A. K. Mohanty, A. Saxena, and S. S. Kapoor, Phys. Rev. C **67**, 041601(R) (2003).